Energy-loss and exit-angle distributions of fragmented H_2^+ ions after traversing carbon foils

Rafael Garcia-Molina,[1] Cristian D. Denton,[1,*] Isabel Abril,[2] and Néstor R. Arista[3]

[1]*Departamento de Física, Universidad de Murcia, Apartado 4021, E-30080 Murcia, Spain*
[2]*Departament de Física Aplicada, Universitat d'Alacant, Apartat 99, E-03080 Alacant, Spain*
[3]*Instituto Balseiro, Centro Atómico Bariloche, RA-8400 Bariloche, Argentina*

We analyze the dependence on the exit angle of the energy loss suffered by the fragment protons resulting from the dissociation of swift H_2^+ molecules after traversing thin carbon foils. The trajectory of each proton was followed by numerically solving the corresponding equations of motion, using the dielectric formalism to describe the forces due to electronic excitations in the medium, whereas the repulsion between protons from the same molecule was taken into account by using a Coulomb potential. Nuclear collisions with target nuclei were incorporated through a Monte Carlo code. The contribution of each one of the above interactions to the joint angle and energy-loss spectra of the fragment protons is discussed as a function of the molecule incident energy and foil thickness.

PACS number(s): 34.50.Bw, 36.40.−c

I. INTRODUCTION

More than twenty years ago, Brandt and co-workers [1] showed both theoretically and experimentally that the motion of a correlated set of ions, resulting from the fragmentation of a molecule when traversing a solid target, opened new possibilities of studying the interaction of charged projectiles with solids. Since then, many phenomena and applications related to the transmission of correlated or uncorrelated swift ions have been observed and devised, such as secondary electron emission [2], charge fractions [3,4], molecular transmission yields [5,6], imaging of the geometrical structure of small molecules [7], determination of the stereochemical structure of molecular ions [8], ionization of target inner shells [9], or fusion studies [10,11], among others.

Most of these phenomena result from the manner in which the ions of the molecule deliver energy to the target, which is substantially different from the sum of energy lost by the same number of ions that form the molecule, interacting individually (i.e., in an uncorrelated way) with the target. The responsible of some of these differences is the vicinage or interference force due to the wake potential induced in the medium by each ion [1,12–16]. Although this wake potential is a function of the projectile velocity and the electronic properties of the target, the interference effects depend on the internuclear separation and on the molecular orientation relative to the projectile motion [17,18].

The aim of this work is to study the energy-loss distributions of the fragment protons resulting from the dissociation of swift H_2^+ projectiles when traversing thin carbon foils. This analysis will be done as a function of the incident energy, foil thickness and exit angle of the fragments.

The paper is organized as follows. In the next section we introduce the theoretical basis of our calculations. The main results of these calculations are discussed in Sec. III, and the final conclusions are presented in Sec. IV.

---

*Permanent address: Instituto Balseiro, Centro Atómico Bariloche, RA-8400 Bariloche, Argentina.

II. CALCULATION PROCEDURE

The goal of our calculation is to find out the exit angle and energy of each proton that compose the H_2^+ molecular ion, after traversing a thin amorphous carbon foil. For this purpose we have developed a code that solves the equation of motion of both protons and follows their trajectories inside the target, taking into account also the plural nuclear scattering with the target nuclei.

The initial configuration of the H_2^+ molecular ion before entering the material is given by two parameters: the initial internuclear distance d and the angle β between the internuclear vector and the direction of motion. Both parameters were chosen by a Monte Carlo code trying to reproduce closely standard experimental situations. The angle β was randomly distributed and the distance d was chosen according to the population of vibrational states of the H_2^+ molecular ion [1,19,20].

When the H_2^+ molecular ion enters into a solid it loses its bound electron in the first atomic layers; the stripping time is typically $\sim 10^{-16}$ s [21]. Then the system becomes a pair of fragment protons that move through the solid in a correlated way. In this situation each proton experiences three main forces, namely: the self-retarding force $\vec{F}_{self-ret}$, the interference force $\vec{F}_{interf}$, and the Coulomb repulsion force $\vec{F}_{Coul}$.

The self retarding force $\vec{F}_{self-ret}$ is the usual stopping force acting on each proton due to the electronic excitations induced in the medium by the passage of the charge. One method to describe these electronic excitations in a realistic way is by means of the dielectric formalism, using a linear combination of Mermin type [22] energy-loss functions to model the dielectric properties of the stopping medium [23–25].

The wake potential generated by each proton also affects the motion of its partner in such a way that the slowing down of two correlated protons is different from the slowing down of two individual protons. The resulting force, called the interference force $\vec{F}_{interf}$, can also be calculated within the dielectric formalism [25,26], and it is very important to de-

scribe correctly the correlated motion of the fragment protons, because it affects their velocities, both in magnitude and direction. As a consequence of the latter there is a tendency to align the internuclear axis with the incident velocity.

The third force acting on the system is the Coulomb repulsion between both protons, which tends to increase the internuclear distance, accelerating the leading proton and stopping the trailing one. This interaction is described by the Coulomb potential.

Therefore, when the fragment protons are inside the material, the total force acting on each proton at a given instant is obtained by the sum of the just mentioned forces

$$\vec{F} = \vec{F}_{self\text{-}ret} + \vec{F}_{interf} + \vec{F}_{Coul} . \tag{1}$$

The classical trajectories of each molecular component can be followed by an integration of the equations of motion of the system. For this purpose we have used a finite difference algorithm, namely the Verlet algorithm [27], and at each time step we have calculated the corresponding force acting on each proton to predict its position and velocity at the next time step. It is important to emphasize that the self-retarding force was chosen randomly at each time step from a Gaussian distribution centered in the stopping power corresponding to the instantaneous velocity of the projectile, and with a width related to the energy-loss straggling. The energy-loss straggling, which was also obtained within the dielectric formalism, allows us to account for the fluctuations in the energy loss due to the statistical nature of the electronic excitations.

The effect of the nuclear collisions with the target atoms was also taken into account via a Monte Carlo (MC) code [28]. In this binary collision model the key parameters are the distance between consecutive nuclear collisions and the angles involved at each collision. The former depends mainly on the atomic density of the target whereas the distribution of polar scattering angles was determined using the universal potential cross section [29] and the MC method.

Once the fragments exit the foil they only interact via the Coulomb repulsion, until their eventual arrival to the detector (considered to be at infinite distance as compared with the target thickness). The trajectory due to this Coulomb repulsion is calculated analytically using energy and Runge-Lentz vector conservation [30]. In this manner we are able to predict in a realistic way the asymptotic velocities of the fragment protons, obtaining the corresponding energy-loss and angle distributions. In the following we use atomic units, except where otherwise stated.

III. ENERGY-LOSS AND EXIT-ANGLE DISTRIBUTIONS

A. Contribution of each interaction

In Fig. 1 we show the joint distribution of energy loss and exit angles of the fragment protons resulting when a H_2^+ beam incides with velocity $v = 5$ a.u. on a 150-a.u.-thick amorphous carbon foil. The thick lines represent the energy-loss distributions at zero angle, whereas the arrows in the energy-loss axis correspond to their mean energy loss. We
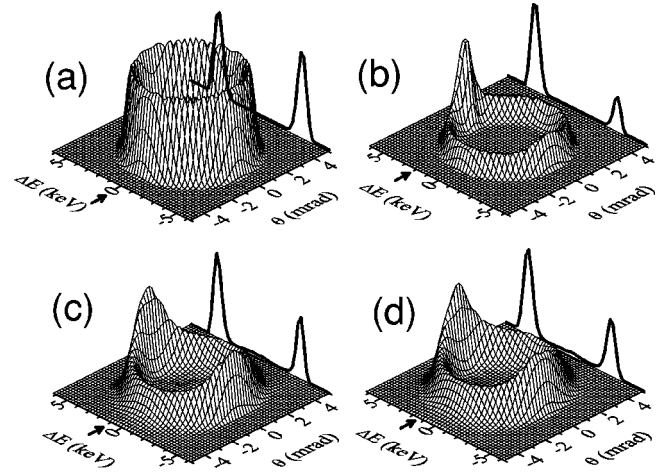

FIG. 1. Joint distribution of energy loss and exit angle of the fragment protons resulting from the dissociation of H_2^+ molecules with $v = 5$ a.u. after traversing a 150 a.u.-thick amorphous carbon foil. The following interactions were taken into account in each case: (a) only the Coulomb explosion; (b) Coulomb explosion and interference effects; (c) Coulomb explosion, interference effects, and nuclear scattering; (d) all the interactions together, including the individual stopping power. The thick curves represent the energy-loss distribution at zero exit angle, whose mean value is indicated by an arrow.

have separated the contribution of each interaction in order to visualize its effect on the distribution. The contribution of the Coulomb explosion is represented in Fig. 1(a), whereas in Fig. 1(b) we have also added the interference effects due to the electronic excitations induced in the solid by the partner proton. The effect of the nuclear collisions were incorporated in Fig. 1(c), and finally in Fig. 1(d) we have added the contribution of the self-retarding force; i.e., the latter figure contains the contributions of all the interactions together.

The Coulomb explosion gives rise to a ring-shaped energy loss and exit angle distribution of constant height [Fig. 1(a)]; this agrees with previous experimental results in gaseous targets where the Coulomb repulsion is the main contribution [8] due to the lack of interference effects. Basically the Coulomb explosion accelerates the leading proton of the molecule and decelerates the trailing one. However, this effect is symmetric, and the energy gain of one proton is compensated by the energy loss of its partner, giving a zero mean energy loss, which is indicated by the arrow.

The interference effects created by each proton are concentrated mainly behind it due to the asymmetric character of the wake potential [25]. As a consequence the trailing proton tends to be aligned with the initial velocity direction more efficiently than the leading one. This produces two asymmetrical peaks in the distribution at zero angle, as it is seen in Fig. 1(b). The mean energy loss of ~ 2 keV, indicated by the arrow, is due mainly to the bigger accumulation of trailing protons at zero angle.

The additional inclusion of the nuclear scattering is shown in Fig. 1(c). Besides the broadening of the angular distribution, there is a partial frustration of the previous alignment correlation, reducing the difference between the magnitude
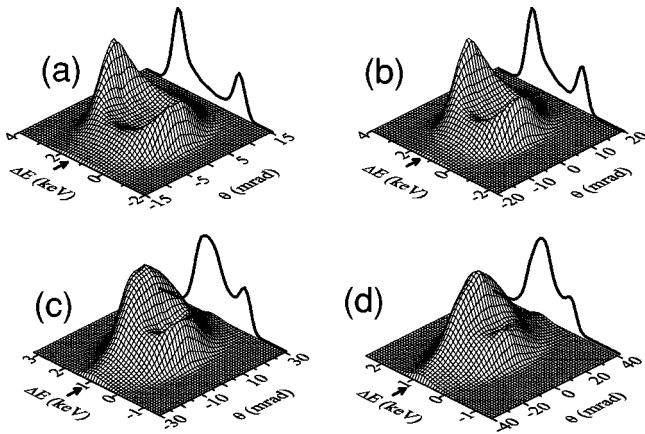
FIG. 2. Joint distribution of energy loss and exit angle of the fragment protons resulting from the dissociation of H_2^+ molecules at different velocities v, after traversing a 150 a.u.-thick amorphous carbon foil. (a) $v = 2$ a.u., (b) $v = 1.79$ a.u., (c) $v = 1.26$ a.u., and (d) $v = 1$ a.u. The thick curves represent the energy-loss distribution at zero exit angle, whose mean value is indicated by an arrow.

of the two peaks at zero angle. Then the mean energy loss at zero angle is reduced compared with Fig. 1(b).

Finally the consideration of the self-retarding force [Fig. 1(d)] makes no changes in the shape of the distribution, except for a shift in the energy-loss scale, which corresponds to the energy loss of a lonely traveling proton. For the projectile velocity discussed here, this energy displacement is rather small (≈ 0.4 keV).

B. Dependence with the projectile velocity and the foil thickness

The evolution of the energy-loss and exit-angle distribution (including all the interactions), when the projectile velocity varies, is shown in Fig. 2 for a constant foil thickness of 150 a.u. We can notice that the angular width of the ring increases with decreasing velocity, whereas the opposite occurs with the energy loss width. This can be understood analyzing the behavior of the Coulomb explosion in the center of mass frame and relating it to magnitudes in the laboratory. The exit angle θ and the energy loss ΔE of each fragment, are related to the velocity v by

$$\theta \approx v_\perp / v, \quad \Delta E \approx m v_\parallel v, \tag{2}$$

where $v_\perp$ and $v_\parallel$ are, respectively, the perpendicular and parallel components of the velocity in the center of mass frame, with respect to the incident direction. For this reason, decreasing v increases the angle θ and decreases the energy loss ΔE. These effects, combined with the increasing contribution of the nuclear collisions to the broadening of the angular distribution and the bigger dwell time at low velocities, distort the ring pattern occurring at high velocities into a hill shaped distribution at low velocities.

Figure 2 clearly shows that the mean energy loss at zero angle is smaller at lower velocities, which is due to two main causes: the velocity dependence of the self-retarding force in this range [25], and the partial loss of correlation between the fragment protons.
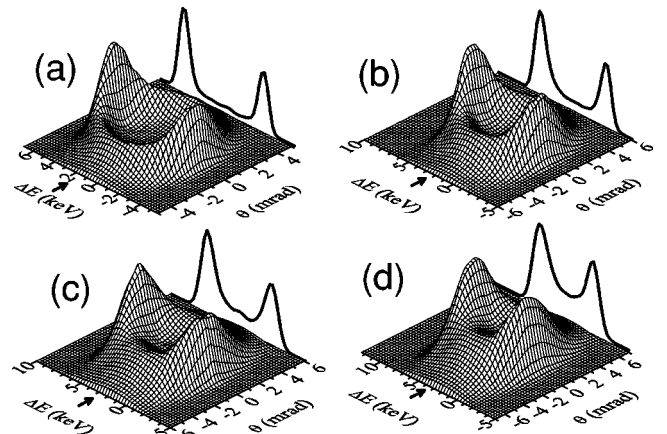

FIG. 3. Joint distribution of exit angle and energy loss of the fragment protons resulting from the dissociation of H_2^+ molecules of velocity $v = 5$ a.u. after traversing amorphous carbon foils of several thicknesses D: (a) $D = 300$ a.u., (b) $D = 500$ a.u., (c) $D = 750$ a.u., and (d) $D = 1000$ a.u. The thick curves represent the energy-loss distribution at zero exit angle, whose mean value is indicated by an arrow.

In Fig. 3 we show the energy-loss and exit-angle distributions of H_2^+ fragments after traversing amorphous carbon foils of different thicknesses D, for an incident velocity $v = 5$ a.u. The shape of the ring depends only on the projectile velocity through Eq. (2), so it remains unchanged, although it is widespread in angles due to nuclear scattering. We can see that this effect is also responsible for the increase of the amount of fragments that lie in the inner part of the ring, as the target thickness grows. As expected, the average energy loss of the distribution (indicated by an arrow) increases with the foil thickness.

In Fig. 4 we compare the experimental [8] and the calculated distribution of energy loss and exit angle of fragment protons for $v = 5.29$ a.u. H_2^+ incident on a 166-a.u.-thick carbon foil. We have drawn our figure in such a manner that the trailing peaks of both, the experimental and the calculated distributions, have the same the height. It can be observed that these distributions are in general good agreement; the widths of the angular distributions are quite similar in both cases, as well as the energy separation between the leading and trailing peaks. Comparison with other experimental data by Golovchenko and Laegsgaard [31], for the
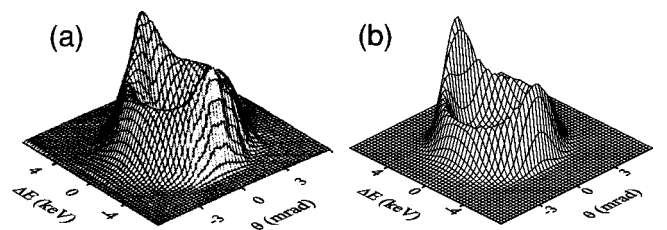

FIG. 4. Comparison between (a) the experimental [8] and (b) the calculated joint distribution of energy loss and exit angle of the fragment protons resulting from the dissociation of $v = 5.29$ H_2^+ molecules in a 166 a.u. thick carbon foil. The experimental figure is reprinted with permission of the American Chemical Society.
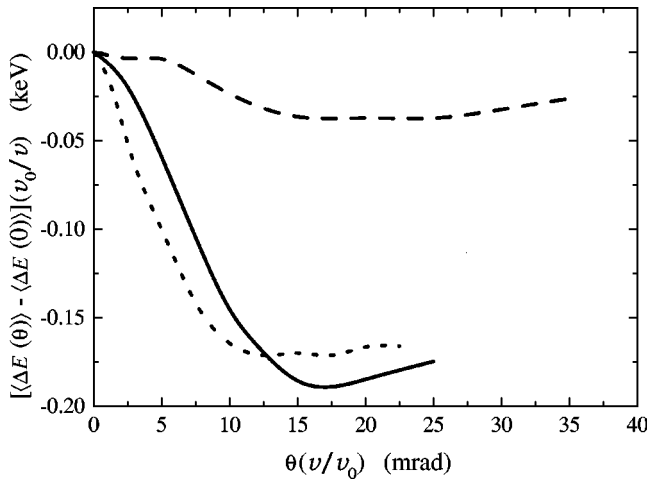
FIG. 5. Mean energy loss of proton fragments, relative to the mean energy loss at zero angle, as a function of their exit angle for a 150 a.u. thick amorphous carbon foil. We have scaled the energy-loss axis by v_0/v and the exit-angle axis by v/v_0, where $v_0 = 1$ a.u. is the Bohr velocity. The dashed line corresponds to $v = 1$ a.u., the solid line to $v = 2$ a.u., and the dotted line to $v = 5$ a.u.

case of $v = 6.3$ a.u. H_2^+ incident on a 190-a.u.-thick carbon foil, also reproduces the main trends of the distribution.

Finally, in Fig. 5 we show the mean energy loss of the proton fragments, relative to the mean energy loss at zero angle, as a function of their exit angle, θ. We display the results for a 150-a.u.-thick amorphous carbon foil and three different projectile velocities ($v = 1, 2$ and 5 a.u.). We have normalized the scales with the incident velocity v in order to show all the results in the same figure. The mean energy loss has a maximum at zero angle and decreases for small values of θ, reaching a minimum for all the velocities analyzed. These results can be explained as due to an acummulation of trailing protons at zero angle, in such a manner that the mean energy loss is displaced towards the trailing peak. After the minimum value is reached, the mean energy loss begins to grow with the exit angle, because the path length traveled by the fragment protons increases. When the velocity of the projectile decreases, our results tend to show a similar behavior to that recently reported by other authors [32], where an increase of the mean energy loss appears for increasing exit angles; this is what one should expect for long dwell times, as in the case of Ref. [32]. The results presented in Fig. 5 correspond to short dwell times, when the internuclear separation is small, and they show that the effects due to the wake are important in the mean energy loss of the fragment

protons as a function of the exit angle; however, these effects are overcome for large dwell times by the path length increase, as already indicated.

IV. CONCLUSIONS

We have developed a code that follows the trajectories of the protons resulting from the dissociation of H_2^+ molecular projectiles traversing amorphous carbon foils. The forces due to the electronic perturbation induced in the medium by the motion of the protons are described by a linear response dielectric theory. A Monte Carlo program was included to take account of the nuclear scattering suffered by each proton when it interacts with the target atomic nuclei. The main features in the joint distribution of energy loss and exit angle of the fragment protons are easily analyzed by separating each contribution of the above mentioned interactions. The following features are observed: (i) the Coulomb explosion between both protons is responsible for the ring shape of the distribution; (ii) the interference effects produce two asymmetric peaks at zero angle due to the alignment tendency of the wake force; (iii) contrary to previous models based on a single plasmon pole approximation, we observe that the asymmetry persists with decreasing velocities down to $v = 1$ a.u.; (iv) the nuclear collisions tend to broaden the angular distribution, contributing to disalign the protons from the incident velocity direction, and, finally, (v) the self-retarding force causes a shift in the mean energy loss of the distribution, as it should be expected.

For a given target thickness, when decreasing the velocity of the molecular beam there is a transition from a ring shaped distribution to a single peaked one with a partial loss of correlation. Nevertheless, at velocities as low as $v = 1$ a.u., there is still evidence of correlation between the protons. At a fixed velocity, increasing the target thickness preserves the size of the ring distribution, but there is a filling of the central part of the ring due to nuclear scattering. For the short dwell times considered here, the mean energy loss of the fragment protons decreases with the exit angle, which is due to the alignment effect of the trailing protons at zero exit angle.

[1] W. Brandt, A. Ratkowski, and R. H. Ritchie, Phys. Rev. Lett. **33**, 1325 (1974).

[2] H. J. Frischkorn, K. O. Groeneveld, P. Koschar, R. Latz, and J. Schader, Phys. Rev. Lett. **49**, 1671 (1982).

[3] B. T. Meggitt, K. G. Harrison, and M. W. Lucas, J. Phys. B **6**, L362 (1973).

[4] V. P. Zaikov, V. N. Novozhilova, I. S. Dmitriev, Ya. A. Teplova, V. S. Nikolaev, and E. I. Sirotinin, Nucl. Instrum. Methods Phys. Res. B **33**, 216 (1988).

[5] W. H. Escovitz, T. R. Fox, and R. Levi-Setti, IEEE Trans. Nucl. Sci. **NS-26**, 1395 (1979).

[6] N. Cue, N. V. Castro-Faria, M. J. Gaillard, J. C. Poizat, J.

Remillieux, D. S. Gemmell, and I. Plesser, Phys. Rev. Lett. **45**, 613 (1980).

[7] Z. Vager, R. Naaman, and E. P. Kanter, Science **244**, 426 (1989).

[8] D. S. Gemmell, Chem. Rev. **80**, 301 (1980).

[9] J. Bausells and N. Barberán, Solid State Commun. **54**, 71 (1985).

[10] C. Deutsch and N. A. Tahir, Phys. Fluids B **4**, 3735 (1992).

[11] E. Nardi, Z. Zinamon, and D. Ben-Hamu, Nuovo Cimento A **106**, 1839 (1993).

[12] W. Brandt and R. H. Ritchie, Nucl. Instrum. Methods **132**, 43 (1976).

[13] N. R. Arista, Phys. Rev. B **18**, 1 (1978).

[14] P. M. Echenique, R. H. Ritchie, and W. Brandt, Phys. Rev. B **20**, 2567 (1979).

[15] G. Basbas and R. H. Ritchie, Phys. Rev. B **18**, 1 (1978).

[16] G. Basbas and R. H. Ritchie, Phys. Rev. A **25**, 1943 (1982).

[17] T. Kaneko, Phys. Rev. A **51**, 535 (1995).

[18] C. D. Denton, I. Abril, F. J. Pérez-Pérez, R. Garcia-Molina, and N. R. Arista, Radiat. Eff. Defects Solids **142**, 223 (1997).

[19] W. L. Walters, D. G. Costello, J. G. Skofronick, D. W. Palmer, W. E. Kane, and R. G. Herb, Phys. Rev. **125**, 2012 (1962).

[20] J. Remillieux, in *Proceedings of the 5th International Congress on Radiation Research*, edited by O. F. Nygaard, H. I. Adler, and W. K. Sinclair (Academic, New York, 1975), p. 302.

[21] J. Remillieux, Nucl. Instrum. Methods **170**, 31 (1980).

[22] N. D. Mermin, Phys. Rev. B **1**, 2362 (1970).

[23] I. Abril, R. Garcia-Molina, and N. R. Arista, Nucl. Instrum. Methods Phys. Res. B **90**, 72 (1994).

[24] D. J. Planes, R. Garcia-Molina, I. Abril, and N. R. Arista, J. Electron Spectrosc. Relat. Phenom. **82**, 23 (1996).

[25] I. Abril, R. Garcia-Molina, C. D. Denton, F. J. Pérez-Pérez, and N. R. Arista, Phys. Rev. A **58**, 357 (1998).

[26] C. D. Denton, R. Garcia-Molina, I. Abril, and N. R. Arista, Nucl. Instrum. Methods Phys. Res. B **135**, 50 (1998).

[27] M. P. Allen and D. J. Tildesley, *Computer Simulation of Liquids* (Oxford University Press, Oxford, 1987).

[28] W. Moller, G. Pospiech, and G. Schrieder, Nucl. Instrum. Methods **130**, 265 (1975).

[29] J. F. Ziegler, J. P. Biersack, and U. Littmark, *The Stopping and Range of Ions in Solids* (Pergamon, New York, 1985), Vol. 1.

[30] D. Zafjman, Phys. Rev. A **42**, 5374 (1990).

[31] J. Golovchenko and E. Laegsgaard, Phys. Rev. A **9**, 1215 (1974).

[32] M. M. Jakas and N. E. Capuj, Phys. Rev. A **54**, 5031 (1996).